

Formation and structural characterization of amino-substituted [3]ferrocenophanes derived from intramolecular Mannich-type coupling reactions at the metallocene framework

Patrick Liptau, Stephanie Knüppel, Gerald Kehr, Olga Kataeva¹, Roland Fröhlich¹, Gerhard Erker*

Organisch-Chemisches Institut der Universität Münster, Corrensstrasse 40, D-48149 Münster, Germany

Received 8 February 2001; received in revised form 5 June 2001; accepted 6 June 2001

Abstract

Treatment of lithium(1-dimethylamino-ethenyl)cyclopentadienide (**5a**) with FeCl₂ generated the corresponding substituted ferrocene (**2a**) that rapidly underwent cyclization in a subsequent Mannich-type condensation reaction to yield the unsaturated dimethylamino-substituted [3]ferrocenophane **3a**. The treatment of 1,1'-diacetylferrocene (**1**) with dimethylamine, diethylamine or piperidine in the presence of TiCl₄ resulted in the formation of the analogously structured functionalized [3]ferrocenophanes **3a–3c**, respectively, by a related intramolecular enamine-condensation pathway (complexes **3a** and **3b** were characterized by X-ray diffraction). Catalytic hydrogenation of **3a–c** in THF at Pd/C gave the corresponding saturated amino-substituted [3]ferrocenophane systems **6a–c**. The catalytic hydrogenation proceeds *trans*-product selectively with *trans-6–cis-6* ratios ranging between ca. 5:1 and 7:1 for these examples (the complexes *trans-6a*·HCl, *trans-6b*, and *trans-6c* were characterized by X-ray crystal structure analysis). Quaternization of **6a** by treatment with methyl iodide followed by the reaction with pyrrolidine led to amine exchange at the [3]ferrocenophane framework with the formation of **6d**. The amine exchange proceeds stereoselectively with a predominant overall retention (the *trans-6d–cis-6d* ratio obtained is again ca. 7:1). The complex *trans-6d* was characterized by X-ray diffraction. © 2001 Published by Elsevier Science B.V.

Keywords: Ferrocenophanes; Ferrocene; Catalytic hydrogenation; Stereochemistry

1. Introduction

Functionalized ferrocenes have become important ligands in catalysis [1]. The examples practically applied are mostly derived from systems exhibiting the simple unbridged ferrocene nucleus. Their bridged [*n*]ferrocenophane analogs constitute interesting alternatives [2]. Therefore, it is of interest to develop additional syntheses to suitably substituted frameworks. *ortho*-Diphenylphosphino-1'-dialkylamino[3]ferrocenophanes have been used successfully as controlling chiral ligands in asymmetric catalysis [2]. These ligand systems were derived from the corresponding 1'-amino-substituted

ferrocenophanes, which in turn were prepared by a conventional five-step synthesis starting from ferrocene carbaldehyde [2–7]. We have now found an alternative route that makes a variety of the amino[3]ferrocenophanes easily available in two steps starting from, e.g. the readily available 1,1'-diacetylferrocene (Chart I).

We have recently reported a novel synthetic entry to unsaturated amino-substituted [3]ferrocenophanes that may provide a broad entry into a variety of functionalized [3]ferrocenophane derivatives [8]. Our synthesis represents an alternative to the elusive aldol condensation reaction for constructing the three-carbon bridge of the unsaturated [3]ferrocenophane framework [9,10]. In our case a suitable 1,1'-diacetylferrocene (e.g. **1**) is converted to the corresponding enamine (**2**) [11] which is then in an acid catalyzed Mannich-type condensation reaction converted to the substituted [3]ferrocenophane derivative (**3**, see Chart II).

* Corresponding author. Tel.: +49-251-8333221; fax: +49-251-8336503.

E-mail address: erker@uni-muenster.de (G. Erker).

¹ X-ray crystal structure analyses.

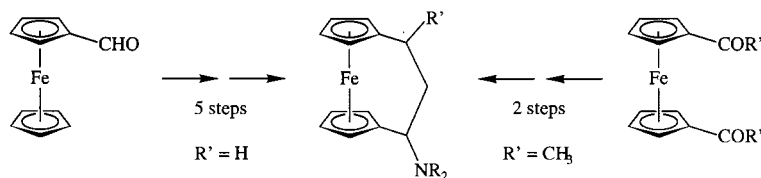


Chart I.

We have now used this and a related entry [12,13] for the synthesis of a variety of examples of the general class of amino-substituted unsaturated [3]ferrocenophanes **3**, and we have used them as starting materials for conversion to saturated amino-substituted [3]ferrocenophane derivatives (**6**), prepared by catalytic hydrogenation and, in some cases, subsequent amine exchange reactions. Both the reaction types proceeded stereoselectively and with remarkable overall diastereoselectivities.

2. Results and discussion

2.1. Synthesis and structural characterization of the unsaturated amino [3]ferrocenophanes **3**

Two routes were employed in the syntheses of the unsaturated amino-functionalized [3]ferrocenophanes that were used as the starting materials for the subsequent hydrogenation reactions. 1,1'-Diacetylferrocene [14] was treated with a large excess of dimethylamine and a stoichiometric quantity of the Lewis acid TiCl_4 in pentane solution [11]. This led to the in situ formation of the corresponding bis-enamine (**2**) that directly underwent the Mannich-type condensation reaction under the influence of the titanium tetrachloride Lewis acid to yield [3]ferrocenophane **3a** (> 80% isolated as an orange crystalline solid). The corresponding diethylamino and the piperidino derivatives, **3b** (present study) and **3c** [8] were synthesized analogously (see Scheme 1).

The dimethylamino[3]ferrocenophane **3a** was also prepared by an alternative route. This started from 6-dimethylamino-6-methylfulvene (**4**) [15]. Treatment with LDA removed a proton from the 6-methyl group to give the enamino-substituted Cp-anion reagent **5** [16], which in turn was reacted with FeCl_2 . Under the applied reaction conditions (12 h in toluene at 60 °C) the in situ generated substituted ferrocene derivative **2a** underwent the Mannich-type condensation reaction to give **3a**, which was isolated in ca. 40% yield from this alternative reaction pathway (see Scheme 1).

The new complexes **3a** and **3b** were characterized spectroscopically and by X-ray crystal structure analyses. An inspection of the molecular structure of complex **3a** (– NMe_2 substituent) reveals that the completely unsaturated three-carbon bridge spans the ferrocene

framework almost ideally. The attachment of the Cp– $\text{C}(\text{sp}^2)$ connections (C1–C6, C11–C8, see Fig. 1) lead only to slight distortions from the typical bond lengths and bond angles (e.g. C1–C6–C7, 122.0(2)°; C11–C8–C7, 123.8(3)°; C6–C7–C8, 130.4(3)°). The metallocene remains almost linear, i.e. in **3a** the Cp(centroid)–Fe–Cp(centroid) angle amounts to 171.5° (the corresponding angle between the best planes of the two $\eta^5\text{-C}_5\text{H}_4$ ligands is found at 12.6°). The enamino-nitrogen atom in complex **3a** is nearly trigonally planar coordinated (sum of C–N–C angles at N9: 355.9°) [17]. The dienamino-bridge in complex **3a** is coplanar oriented, and it exhibits an alternating array of C–C single and double bonds inside the conjugated π -system (C10–C6, 1.342(4) Å; C6–C7, 1.453(4) Å; C7–C8, 1.350(4) Å; C8–N9, 1.383(4) Å) [18].

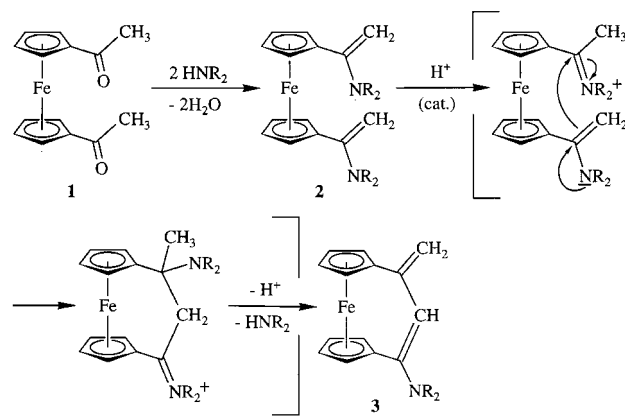
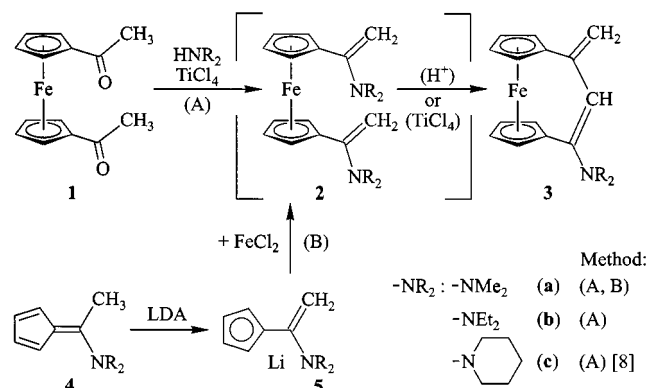


Chart II.



Scheme 1.

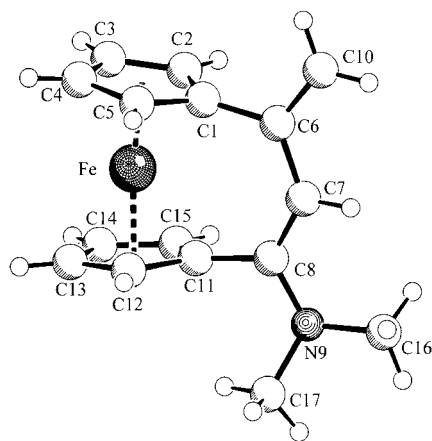


Fig. 1. Side view of the molecular structure of the dimethylamino [3]ferrocenophane (**3a**). Selected bond lengths (Å) and bond angles (°): Fe–C_{Cp} 1.987(3)–2.056(3), C_{Cp}–C_{Cp} 1.411(4)–1.432(4), C1–C6 1.497(4), C6–C10 1.342(4), C6–C7 1.453(4), C7–C8 1.350(4), C8–N9 1.383(4), N9–C16 1.453(4), N9–C17 1.448(4); D_{Cp}–Fe–D_{Cp} 171.5, C1–C6–C7 122.0(2), C1–C6–C10 117.3(3), C10–C6–C7 120.6(3), C6–C7–C8 130.4(3), C7–C8–N9 122.8(3), C7–C8–C11 123.8(3), C11–C8–N9 113.3(2), C8–N9–C16 119.9(2), C8–N9–C17 120.9(2).

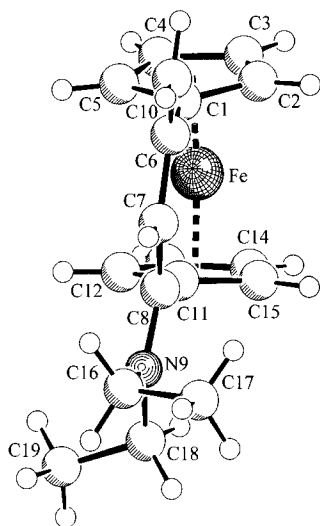


Fig. 2. A projection of the molecular geometry of complex **3b** in the solid state. Selected bond lengths (Å) and bond angles (°): Fe–C_{Cp} 1.985(2)–2.062(2), C_{Cp}–C_{Cp} 1.414(4)–1.430(3), C1–C6 1.486(3), C6–C10 1.341(3), C6–C7 1.453(3), C7–C8 1.364(3), C8–N9 1.380(3), N9–C16 1.455(3), N9–C18 1.464(3); D_{Cp}–Fe–D_{Cp} 171.2, C1–C6–C7 122.5(2), C1–C6–C10 116.6(2), C10–C6–C7 120.9(2), C6–C7–C8 130.2(2), C7–C8–N9 122.9(2), C7–C8–C11 123.1(2), C11–C8–N9 114.0(2), C8–N9–C16 121.3(2), C8–N9–C18 123.3(2).

The bridgeside-view of the structure of complex **3b** (see Fig. 2) shows that the complexes **3** contain a nearly C_s symmetric carbon framework (although not crystallographically exact). This even extends to the α-carbon atoms of the ethyl substituents bonded to nitrogen (N9); as expected, a conformational situation is found where the adjacent ethyl-CH₃ groups are oriented toward opposite sides from the idealized central molecu-

lar plane. Again, the slight bending of the Cp–Fe–Cp framework can be seen from the projection of the molecule of **3b** as shown in Fig. 2.

2.2. Catalytic hydrogenation: formation and structural characterization of the [3]ferrocenophane derivatives **6**

Catalytic hydrogenation of the complexes **3a–c** was carried out in THF at ambient temperature and ambient pressure. Hydrogen uptake was followed by means of a gas burette.

Complete and selective hydrogenation of both C=C double bonds of the doubly unsaturated dienamine-type bridge was observed under these conditions. The reaction was completed after ca. 1 h (employing 1 mmol amounts of **3** in ca. 50 ml of THF).

In principle two stereoisomers (*trans*-**6**, *cis*-**6**) can be formed in this reaction characterized by a relative *trans*- or *cis*-attachment of the methyl and –NR₂ substituents at the saturated C₃ bridge of the [3]ferrocenophane framework. In the three hydrogenation examples investigated in this study, the *trans*-disubstituted products *trans*-**6(a–c)** are obtained predominantly [*trans*–*cis* ratio = 6.7:1 (**6a**, R = –NMe₂); 4.7:1 (**6b**, R = –NEt₂), 6.6:1 (**6c**, –NC₅H₁₀)]. The *trans*–*cis* ratio can be measured readily by ¹H-NMR using the well-separated resonances of the 8-H hydrogen atom or in some cases the methyl signals of the respective stereoisomers (i.e. the signal of the C–H unit of the bridge adjacent to nitrogen).

We tried to get single crystals of complex **6a** (–NMe₂) for an X-ray crystal structure determination, but were only able to isolate its hydrochloride **6a**·HCl in a suitable crystalline form. Single crystals of the ammonium salt **6a**·HCl were obtained by the slow evaporation of a dichloromethane-*d*₂ solution of **6a**.

The view of the molecular geometry of **6a**·HCl (see Fig. 3) reveals the presence of a strongly folded C₃ bridge of the [3]ferrocenophane framework [2]. The C5–C1–C6–C7–C8–C11–C12 frame in its saturated part resembles a boat-shaped conformation similar to the conformation found in the hydrocarbon cycloheptane [19]. The C5–C1–C6–C7 dihedral angle amounts to 68.9(3)° (analogously: C12–C11–C8–C7 is –41.1(3)°, and θ C1–C6–C7–C8 is 60.3(2)° (C11–C8–C7–C6 is –76.9(2)°). This specific conformational shape of the **6a**·HCl framework leads to a pronounced differentiation of the substituent positions at the sp³-hybridized carbon atoms C6, C7, and C8 into axial and equatorial orientations. The X-ray crystal structure analysis of complex **6a**·HCl shows a *trans*-arrangement of the 6-CH₃ and the 8-NMe₂H⁺ substituents at the metallacyclic ring, and a conformation, that has the 6-CH₃ substituent oriented axially, whereas the 8-NMe₂H⁺ group is positioned equatorially. Consequently, the observed conformation of the *major* diastereoisomer (see

below) of **6a**·HCl exhibits dihedral angles of $-67.7(2)^\circ$ (C10–C6–C7–C8) and $156.3(2)^\circ$ (C6–C7–C8–N9) that characterizes this specific conformational arrangement in the solid state.

The major stereoisomer of the free amine **6a** in solution also exhibits the 6-CH₃ and 8-NMe₂ substituents *trans*-positioned at the ring, i.e. corresponds to the structure of *trans*-**6a**·HCl that was characterized by

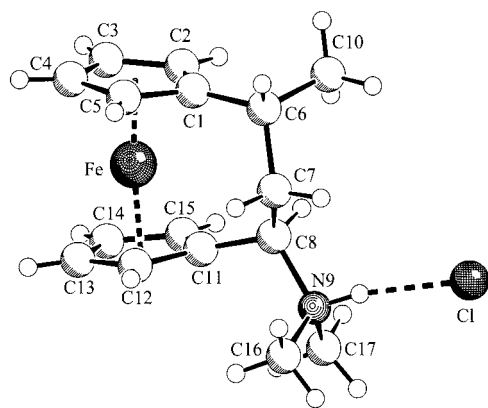


Fig. 3. Molecular structure of *trans*-**6a**·HCl (major isomer). Selected bond lengths (Å) and bond angles ($^\circ$): Fe–C_{Cp} 1.997(2)–2.056(2), C_{Cp}–C_{Cp} 1.409(4)–1.431(3), C1–C6 1.518(3), C6–C10 1.522(3), C6–C7 1.543(3), C7–C8 1.538(3), C8–N9 1.527(2), N9–C16 1.483(3), N9–C17 1.484(3), N9–H9 0.91, H9···Cl 2.10, N9···Cl 2.997; D_{Cp}–Fe–D_{Cp} 173.4, C1–C6–C7 113.1(2), C1–C6–C10 112.2(2), C10–C6–C7 112.1(2), C6–C7–C8 112.9(2), C7–C8–N9 109.9(2), C7–C8–C11 114.7(2), C11–C8–N9 111.7(2), C8–N9–C16 115.0(2), C8–N9–C17 110.6(2), N9–H9···Cl 169.

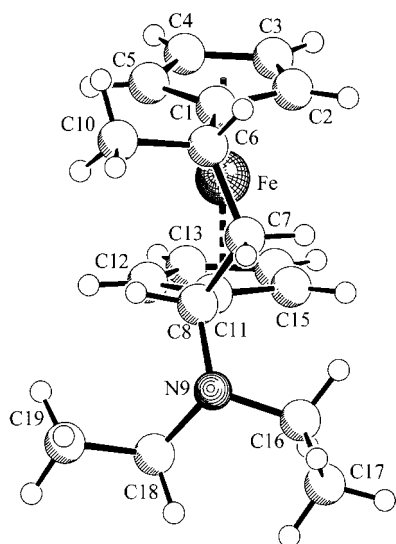
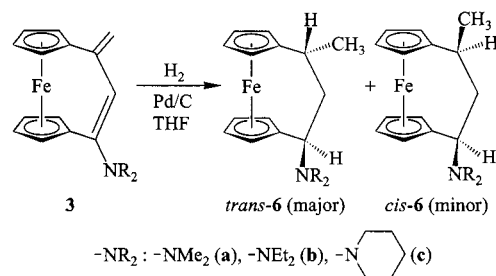


Fig. 4. A projection of the molecular structure of the complex *trans*-**6b**. Selected bond lengths (Å) and bond angles ($^\circ$): Fe–C_{Cp} 2.012(2)–2.056(2), C_{Cp}–C_{Cp} 1.413(4)–1.429(3), C1–C6 1.513(3), C6–C10 1.518(3), C6–C7 1.544(3), C7–C8 1.531(3), C8–N9 1.475(3), N9–C16 1.470(3), N9–C18 1.460(3); D_{Cp}–Fe–D_{Cp} 173.0, C1–C6–C7 112.4(2), C1–C6–C10 112.1(2), C10–C6–C7 113.1(2), C6–C7–C8 114.9(2), C7–C8–N9 111.1(2), C7–C8–C11 112.1(2), C11–C8–N9 115.2(2), C8–N9–C16 113.9(2), C8–N9–C18 112.5(2).



Scheme 2.

X-ray diffraction (see above). This has become evident by the ¹H-NMR analysis of the major **6a** isomer in CD₂Cl₂. A characteristic set of *J*(H,H) coupling constants was obtained indicating an antiperiplanar arrangement of the hydrogen atoms 8-H and 7-H_{ax} (³*J*(8-H, 7-H_{ax}) = 10.5 Hz, ²*J*(7-H_{ax}, 7-H_{eq}) = 13.5 Hz) and a *gauche* arrangement of 7-H_{ax} with 6-H [³*J*(7-H_{ax}, 6-H) = 3.8 Hz; ³*J*(7-H_{eq}, 6-H) = 3.3 Hz; atom numbering as in Fig. 3).

A closely analogous situation is observed for the diethylamino-substituted [3]ferrocenophane **6b**. The major isomer again has the –NR₂ group oriented in an equatorial position at the framework (¹H-NMR (CD₂Cl₂): δ = 3.47 (8-H, ³*J*(8-H, 7-H_{ax}) = 11.4 Hz, ³*J*(8-H, 7-H_{eq}) = 2.4 Hz). The structural assignment was supported by the results of an X-ray crystal structure determination. Single crystals of the major *trans*-**6b** isomer were obtained from pentane. The projection depicted in Fig. 4 shows a view of the folded substituted trimethylene chain of the [3]ferrocenophane derivative *trans*-**6b** from its bridged side. The mono-substituted η⁵-Cp ring systems are arranged almost parallel to each other (angle between the best Cp planes is 9.5°; Cp(centroid)–Fe–Cp(centroid) angle is 173.0°). This view shows the axial arrangement of the 6-CH₃ group with its C6–C10 vector oriented almost parallel with the adjacent Cp plane (dihedral angle C5–C1–C6–C10 $-13.0(3)^\circ$). In contrast, the 8-NEt₂ substituent is oriented equatorially at the framework (dihedral angle C15–C11–C8–N9 $-77.6(3)^\circ$). The amino-nitrogen atom in complex *trans*-**6b** is pyramidalized (bond angles C8–N9–C18, 112.5(2)°; C8–N9–C16, 113.9(2)°; C16–N9–C18, 110.6(2)°).

Hydrogenation of the previously reported [3]ferrocenophane system **3c** (see Schemes 1 and 2) gave the piperidino-substituted complex **6c** as a mixture of *trans*- and *cis*-isomers in a 6.6:1 ratio (total yield 95%). Again, the major isomer has the 6-CH₃ and 8-amino substituents *trans*-positioned. In solution, the 6-CH₃ group of the major isomer (*trans*-**6c**) is conformationally arranged axially as judged from the typical appearance of the corresponding section of the ¹H-NMR spectrum ((toluene-*d*₈, 600 MHz): δ = 2.99 (8-H), 2.19 (7-H_{ax}), 1.87 (7-H_{eq}), 2.49 (6-H)) which shows a very

characteristic set of coupling constants ($^3J(8\text{-H}, 7\text{-H}_{\text{ax}}) = 10.9$ Hz, $^3J(8\text{-H}, 7\text{-H}_{\text{eq}}) = 2.2$ Hz, $^2J(7\text{-H}_{\text{ax}}, 7\text{-H}_{\text{eq}}) = 13.3$ Hz, $^3J(7\text{-H}_{\text{ax}}, 6\text{-H}) = 2.2$ Hz, $^3J(7\text{-H}_{\text{eq}}, 6\text{-H}) = 4.6$ Hz).

Complex *trans*-**6c** was also characterized by X-ray crystal structure determination (see Fig. 5). It supports the configurational and conformational assignments made (see above). The top view presented in Fig. 5 visualizes the folded geometry of the three-carbon bridge in these systems.

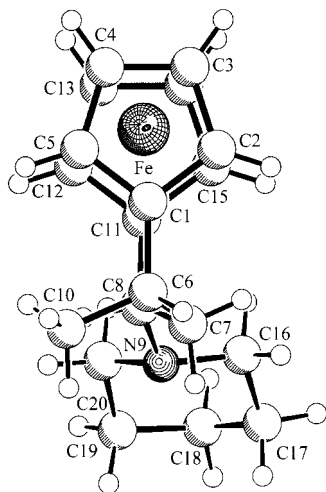
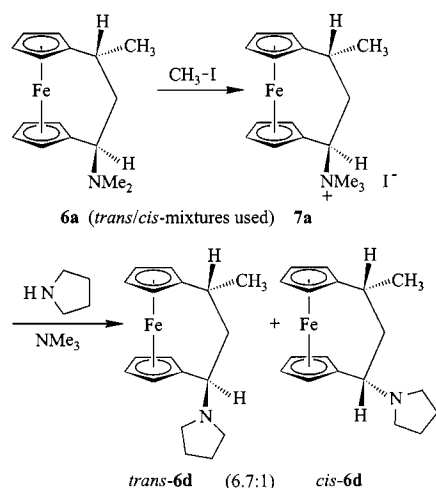


Fig. 5. Top projection of the molecular structure of complex *trans*-**6c**. Selected bond lengths (Å) and bond angles (°) (averaged values from two independent molecules): Fe–C_{Cp} 2.017(4)–2.060(4), C_{Cp}–C_{Cp} 1.406(5)–1.440(5), C1–C6 1.506(5), C6–C10 1.515(5), C6–C7 1.548(5), C7–C8 1.527(5), C8–N9 1.477(4), N9–C16 1.462(4), N9–C20 1.466(4); D_{Cp}–Fe–D_{Cp} 172.6, C1–C6–C7 112.8(3), C1–C6–C10 112.3(3), C10–C6–C7 111.9(3), C6–C7–C8 114.4(3), C7–C8–N9 111.3(3), C7–C8–C11 113.0(3), C11–C8–N9 114.7(3), C8–N9–C16 114.5(2), C8–N9–C20 111.6(2).



Scheme 3.

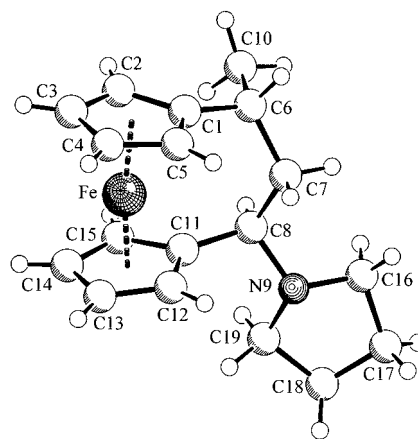


Fig. 6. A view of the molecular structure of the product *trans*-**6d**. Selected bond lengths (Å) and bond angles (°): Fe–C_{Cp} 2.012(2)–2.057(2), C_{Cp}–C_{Cp} 1.417(3)–1.430(3), C1–C6 1.513(3), C6–C10 1.523(3), C6–C7 1.539(3), C7–C8 1.540(3), C8–N9 1.469(2), N9–C16 1.466(3), N9–C19 1.465(3); D_{Cp}–Fe–D_{Cp} 172.3, C1–C6–C7 112.7(2), C1–C6–C10 112.1(2), C10–C6–C7 112.4(2), C6–C7–C8 116.9(2), C7–C8–N9 110.2(2), C7–C8–C11 113.0(2), C11–C8–N9 108.3(2), C8–N9–C16 114.9(2), C8–N9–C19 112.0(2).

2.3. Amine exchange

The [3]ferrocenophanyl amines **6** readily form ammonium salts, that can be employed in amine exchange reactions [21]. Here is a typical example. The dimethyl-amino-substituted [3]ferrocenophane system **6a** was treated with excess methyl iodide in acetonitrile. The in situ generated quaternary ammonium salt **7a** (see Scheme 3) was then directly reacted with pyrrolidine in a concentrated acetonitrile solution. Conventional workup gave the respective *N*-pyrrolidino-substituted [3]ferrocenophane system **6d** in >95% yield. Two isomers were formed in a 6.7:1 ratio. The major isomer in solution was identified as *trans*-**6d** by $^1\text{H-NMR}$ spectroscopy ((CD₂Cl₂, 600 MHz): $\delta = 2.90$ (8-H), 2.29 (7-H_{ax}), 2.21 (7-H_{eq}), 2.66 (6-H)). The characteristic coupling constants could be determined from these spectra using homodecoupling experiments ($^3J(8\text{-H}, 7\text{-H}_{\text{ax}}) = 9.5$ Hz, $^3J(8\text{-H}, 7\text{-H}_{\text{eq}}) = 2.5$ Hz, $^2J(7\text{-H}_{\text{ax}}, 7\text{-H}_{\text{eq}}) = 13.5$ Hz, $^3J(7\text{-H}_{\text{ax}}, 6\text{-H}) = 3.3$ Hz, $^3J(7\text{-H}_{\text{eq}}, 6\text{-H}) = 5.5$ Hz, $^3J(6\text{-H}, 6\text{-CH}_3) = 7.3$ Hz).

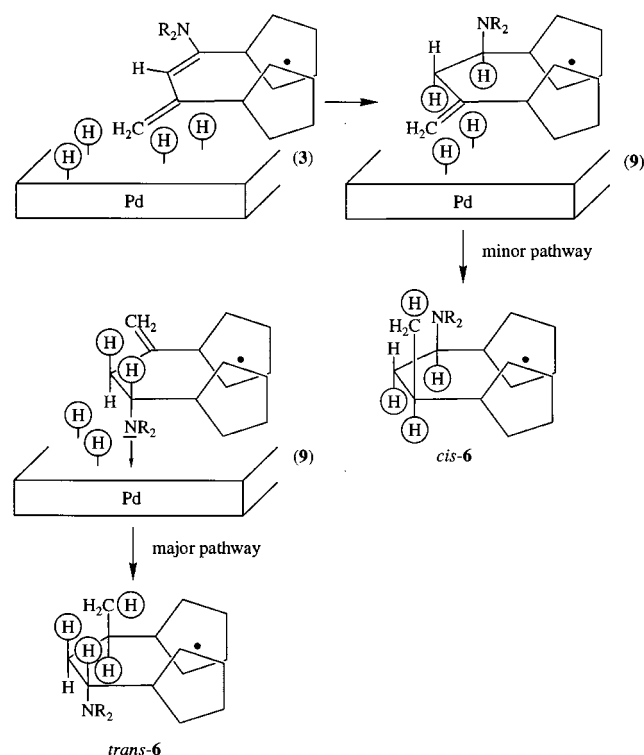
The assignment of the major diastereomeric product as *trans*-**6d** was confirmed by X-ray crystal structure analysis (single crystals from pentane). Inspection of the molecular structure (see Fig. 6) shows the typical folded conformation that leads to a strong orientational differentiation of the geminal groups at the sp³-carbon centers of the bridge. It can be seen from Fig. 6 that the 6-CH₃ group is again oriented in an axial position, whereas the 8-amino substituent, that is attached *trans* to the 6-methyl substituent, is oriented equatorially. The amine exchange reaction at the [3]ferrocenophane framework of **7** proceeds with an overall retention of

stereochemistry, analogous with the general observation made for the related non-bridged aminoalkyl-ferrocene systems [22,23], and for several 1'-amino[3]ferrocenophane derivatives [3,6,24].

2.4. Conclusions

The 1,3-*trans*-disubstituted [3]ferrocenophane derivatives (*trans*-**6**) are formed preferentially by the catalytic hydrogenation of **3** under heterogeneous conditions. This may be rationalized potentially in the following way. Let us assume that the adsorption of the prochiral starting material **3** to the catalyst surface would be followed by the delivery of all the four hydrogen atoms to the doubly unsaturated [3]ferrocenophane. Complete hydrogenation would then be carried out from one enantiotopic face of **3** only, which must result in a selective conversion to *cis*-**6**. This is not observed experimentally. We, therefore, assume that the catalytic hydrogenation kinetically proceeds in a stepwise manner, where after the hydrogenation of one C=C double bond dissociation, rechemisorption may occur allowing the observed enantiofacial alternation in the attack on **3** (Scheme 4).

A *trans*-selective outcome of the hydrogenation reaction would be rationalized by, e.g. assuming that the endocyclic C=C double bond is hydrogenated first. The resulting intermediate then appears to prefer reorientation (probably proceeded by dissociation from the cata-



Scheme 4.

lyst surface followed by readdition) of the substrate from the -NR_2 substituent side, potentially making use of the coordinating abilities of this functional group. In the subsequent step, H_2 is consequently transferred from the surface to the face *cis* to the amino group. This pathway would directly result in the formation of the observed major hydrogenation product *trans*-**6**. Such a two-step hydrogen delivery process seems to constitute the predominant pathway, but not the only one as we have observed that the competing pathways that lead to the *cis*-**6** diastereoisomers are still inside the range of the experimentally observed competing reaction routes.

We have developed a short synthetic pathway to substituted amino-[3]ferrocenophane systems **6**, and we have characterized the diastereoselective outcome of their formation and of a subsequent interconversion. This may open alternative pathways to prepare useful ligand systems based on [3]ferrocenophane chemistry. Such studies are being actively pursued in our laboratory.

3. Experimental

Reactions were carried out under argon using Schlenk-type glassware or in a glovebox. Solvents were dried and distilled under argon prior to use. NMR spectra were measured on a Varian UNITY Plus (^1H : 599.8; ^{13}C : 150.8 MHz) or a Bruker AC200P NMR spectrometer (^1H : 200; ^{13}C : 50 MHz). Most assignments were secured by a combination of 1D and 2D NMR experiments [25]. The melting points (m.p.) given were obtained by DSC. The starting material 1,1'-diacetylferrocene (**1**) [14] and the unsaturated piperidino[3]ferrocenophane (**3c**) [8] were prepared according to the procedures outlined in the literature.

3.1. Preparation of complex **3a**

Method A: dimethylamine (20.0 g, 440 mmol) was condensed at -78°C and dissolved in 50 ml of pentane at low temperature. The resulting solution was transferred to a cooled suspension of 4.0 g of 1,1'-diacetylferrocene **1** (14.8 mmol) in 80 ml of pentane. Over a period of 20 min, a solution of 2.0 ml TiCl_4 (17.8 mmol) in 20 ml of pentane was added to this mixture. The orange suspension was allowed to warm up to room temperature (r.t.) and then stirred for 5 h. The precipitate formed was removed by filtration and the solvent was then evaporated from the clear orange filtrate in vacuo to yield 3.3 g of orange crystals of **3a** (81%). Crystals suitable for the X-ray structure analysis were grown from pentane.

Method B: the reagent **5** (1.0 g, 7.08 mmol) was suspended in 40 ml of toluene. Solid FeCl_2 (449 mg,

3.54 mmol) was added as a single portion to the suspension with rapid stirring at ambient temperature. The mixture was stirred for 12 h at 60 °C. The precipitate formed was removed by filtration. Solvent was removed from the filtrate in vacuo. Recrystallization of the remaining solid from Et₂O gave 404 mg (41%) of complex **3a** as orange–brown solid. HRMS Found: 279.0702. Calc. for C₁₆H₁₇NFe: 279.0710. ¹H-NMR (CDCl₃): δ = 5.47 (s, 1H, 7-H), 5.02 (d, 1H, ²J = 2 Hz) and 4.68 (d, 1H, ²J = 2 Hz, =CH₂), 4.23 (m, 2H, Cp–H), 4.17 (m, 4H, Cp–H), 4.09 (m, 2H, Cp–H), 2.69 (s, 6H, N(CH₃)₂). ¹³C-NMR (CDCl₃): δ = 145.9, 142.0 (C6, C8), 109.7, 108.9 (C7, C10), 90.2, 85.2 (C1, C11), 71.3, 70.0, 69.7, 69.5 (C2–C5, C12–C15), 40.8 (N(CH₃)₂).

3.1.1. X-ray crystal structure analysis of **3a**

Formula C₁₆H₁₇NFe, *M* = 279.16, red–yellow crystal 0.35 × 0.20 × 0.05 mm, *a* = 7.774(1), *b* = 6.078(1), *c* = 26.906(1) Å, β = 90.97(1)°, *V* = 1271.1(3) Å³, ρ_{calc} = 1.459 g cm⁻³, μ = 11.66 cm⁻¹, empirical absorption correction via SORTAV (0.686 ≤ *T* ≤ 0.944), *Z* = 4, monoclinic, space group *P*2₁/*c* (No. 14), λ = 0.71073 Å, *T* = 198 K, ω and φ scans, 7966 reflections collected (± *h*, ± *k*, ± *l*), [(sin θ)/λ] = 0.66 Å⁻¹, 2847 independent (*R*_{int} = 0.058) and 1841 observed reflections [*I* ≥ 2σ(*I*)], 165 refined parameters, *R* = 0.048, *wR*² = 0.083, maximum residual electron density 0.31 (−0.49) e Å⁻³, hydrogens calculated and refined as riding atoms.

3.2. Hydrogenation of **3a**, preparation of complex **6a**

A suspension of 2.5 g (9.0 mmol) of **3a** and 111 mg of Pd/C catalyst (10% Pd) in 80 ml of THF was stirred vigorously at r.t. and hydrogenated at normal pressure for 2 h using a gas-burette. The reaction mixture was filtered. The solvent was removed in vacuo from the filtrate to yield 2.46 g of **6a** (*trans*-**6a**–*cis*-**6a** = 6.7:1 as orange crystals (96%), m.p. (dec.): 62 °C (DSC). Slow evaporation of a saturated solution of **6a** in CD₂Cl₂ gave crystals of *trans*-**6a**·HCl suitable for X-ray crystal structure analysis. *trans*-**6a**: ¹H-NMR (CD₂Cl₂): δ = 4.21 (m, 1H, Cp–H), 4.15 (m, 1H, Cp–H), 4.10 (m, 1H, Cp–H), 4.08 (m, 1H, Cp–H), 4.03 (m, 1H, Cp–H), 4.02 (m, 1H, Cp–H), 4.01 (m, 1H, Cp–H), 3.93 (m, 1H, Cp–H), 3.05 (d, 1H, ³J = 10.5 Hz, 8-H), 2.70 (m, 1H, 6-H), 2.38 (m, 1H, ²J = 13.5 Hz, ³J = 10.5, 3.8 Hz, 7-H_{ax}), 2.20 (s, 6H, 16/17-H), 2.08 (m, 1H, ²J = 13.5 Hz, ³J = 4.6, 3.3 Hz, 7-H_{eq}), 1.33 (d, 3H, ³J = 7.3 Hz, 10-H). ¹³C-NMR (CD₂Cl₂): δ = 92.8 (C-1), 80.5 (C-11), 71.8, 70.0, 69.5, 69.0, 68.9, 68.6, 68.0, 67.7 (C-2/C-3/C-4/C-5/C-12/C-13/C-14/C-15), 59.7 (C-8), 46.2 (C-16/C-17) 42.1 (C-7), 27.9 (C-6), 17.3 (C-10). Anal. Found: C, 67.70; H, 7.48; N, 4.89. Calc. for C₁₆H₂₁NFe (MW 283.2): C, 67.86; H, 7.47; N, 4.95%.

3.2.1. X-ray crystal structure analysis of *trans*-**6a**·HCl

Formula C₁₆H₂₂NFeCl, *M* = 319.65, orange crystal 0.25 × 0.20 × 0.20 mm, *a* = 12.004(1), *b* = 10.245(1), *c* = 13.389(1) Å, β = 113.35(1)°, *V* = 1511.7(2) Å³, ρ_{calc} = 1.404 g cm⁻³, μ = 11.60 cm⁻¹, empirical absorption correction via SORTAV (0.760 ≤ *T* ≤ 0.801), *Z* = 4, monoclinic, space group *P*2₁/*n* (No. 14), λ = 0.71073 Å, *T* = 198 K, ω and φ scans, 12145 reflections collected (± *h*, ± *k*, ± *l*), [(sin θ)/λ] = 0.65 Å⁻¹, 3705 independent (*R*_{int} = 0.046) and 2648 observed reflections [*I* ≥ 2σ(*I*)], 178 refined parameters, *R* = 0.038, *wR*² = 0.070, maximum residual electron density 0.37 (−0.37) e Å⁻³, hydrogen at nitrogen from difference Fourier, others calculated and all refined as riding atoms.

3.3. Synthesis of complex **3b**

A solution of 1 ml TiCl₄ (8.8 mmol) in 20 ml of pentane was added to an ice cold suspension of 2.0 g of **1** (7.4 mmol) and 6.2 ml diethylamine (60 mmol) in 70 ml of pentane over a period of 20 min. The ice bath was then removed and the resulting mixture stirred overnight. The precipitate formed was removed by filtration and the solvent was then removed from the clear red filtrate in vacuo to yield 0.67 g (30%) of red crystalline **3b**. Recrystallization from pentane gave red crystals that were suitable for the X-ray crystal structure analysis, m.p.: 68 °C (DSC). ¹H-NMR (CD₂Cl₂): δ = 5.45 (s, 1H, 7-H), 4.91 (d, 1H, ²J = 2.4 Hz, 10-H), 4.55 (d, 1H, ²J = 2.4 Hz, 10-H), 4.21 (m, 2H, Cp–H), 4.20 (m, 2H, Cp–H), 4.16 (m, 2H, Cp–H), 4.09 (m, 2H, Cp–H), 3.11 (q, 4H, ³J = 7.2 Hz, 16/19-H), 1.03 (t, 6H, ³J = 7.2 Hz, 17/18-H). ¹³C{¹H}-NMR (CD₂Cl₂): δ = 144.4 (C-8), 143.0 (C-6), 108.1 (C-10), 107.7 (C-7), 90.2 (C-1), 84.5 (C-11), 71.8, 70.3, 69.9, 69.8 (C-2/C-3/C-4/C-5/C-12/C-13/C-14/C-15), 43.9 (C-16/C-19), 12.9 (C-17/C-18). Anal. Found: C, 69.92; H, 6.86; N, 4.27. Calc. for C₁₈H₂₁NFe (MW 307.2): C, 70.37; H, 6.89; N, 4.56%.

3.3.1. X-ray crystal structure analysis of **3b**

Formula C₁₈H₂₁NFe, *M* = 307.21, red–yellow crystal 0.30 × 0.25 × 0.05 mm, *a* = 20.176(1), *b* = 10.554(1), *c* = 15.134(1) Å, β = 112.27(1)°, *V* = 2982.2(4) Å³, ρ_{calc} = 1.368 g cm⁻³, μ = 10.01 cm⁻¹, empirical absorption correction via SORTAV (0.753 ≤ *T* ≤ 0.952), *Z* = 8, monoclinic, space group *C*2/*c* (No. 15), λ = 0.71073 Å, *T* = 198 K, ω and φ scans, 11 238 reflections collected (± *h*, ± *k*, ± *l*), [(sin θ)/λ] = 0.66 Å⁻¹, 3551 independent (*R*_{int} = 0.052) and 2737 observed reflections [*I* ≥ 2σ(*I*)], 183 refined parameters, *R* = 0.040, *wR*² = 0.085, maximum residual electron density 0.42 (−0.44) e Å⁻³, hydrogens calculated and refined as riding atoms.

3.4. Hydrogenation of **3b**, preparation of complex **6b**

A suspension of 0.65 g (2.1 mmol) of **3b** and 35 mg Pd/C catalyst (10% Pd) in 30 ml of THF was vigorously stirred at r.t. and hydrogenated for 2 h and filtered subsequently. Evaporation of the solvent from the filtrate afforded a red solid. Recrystallization from pentane yielded 0.30 g (45%) of **6b** (*trans-6b*–*cis-6b* = 4.7:1), m.p.: 74 °C (DSC). Crystals suitable for the X-ray crystal structure analysis were grown from pentane. *trans-6b*: ¹H-NMR (CD₂Cl₂): δ = 4.21 (m, 1H, Cp–H), 4.18 (m, 1H, Cp–H), 4.12 (m, 1H, Cp–H), 4.08 (m, 1H, Cp–H), 4.05 (m, 1H, Cp–H), 4.04 (m, 1H, Cp–H), 4.02 (m, 1H, Cp–H), 3.94 (m, 1H, Cp–H), 3.47 (dd, 1H, ³J = 11.4, 2.4 Hz, 8-H), 2.75 (m, 1H, 6-H), 2.63 (m, 2H, 16/19-H), 2.48 (m, 1H, 7-H_{ax}), 2.34 (m, 2H, 16/19-H), 2.01 (m, 1H, 7-H_{eq}), 1.26 (d, 3H, ³J = 7.2 Hz, 10-H), 1.01 (t, 6H, ³J = 6.6 Hz, 17/18-H). ¹³C{¹H}-NMR (CD₂Cl₂): δ = 93.2 (C-1), 81.9 (C-11), 71.7, 69.4, 69.1, 68.6, 68.5, 68.0, 67.6, 67.1 (C-2/C-3/C-4/C-5/C-12/C-13/C-14/C-15), 52.8 (C-8), 46.9 (C-7), 44.5 (C-16/C-19), 28.2 (C-6), 17.2 (C-10), 13.6 (C-17/C-18). HRMS (ESI) Found 312.1420. Calc. for **6b**·H⁺ (C₁₈H₂₆NFe): 312.1415.

3.4.1. X-ray crystal structure analysis of *trans-6b*

Formula C₁₈H₂₅NFe, *M* = 311.24, yellow crystal 0.40 × 0.35 × 0.25 mm, *a* = 13.385(1), *b* = 7.441(1), *c* = 15.627(1) Å, β = 92.05(1)°, *V* = 1555.4(3) Å³, ρ_{calc} = 1.329 g cm⁻³, μ = 9.60 cm⁻¹, empirical absorption correction via SORTAV (0.700 ≤ *T* ≤ 0.795), *Z* = 4, monoclinic, space group *P*2₁/*c* (No. 14), λ = 0.71073 Å, *T* = 198 K, ω and φ scans, 11 450 reflections collected (±*h*, ±*k*, ±*l*), [(sin θ)/λ] = 0.66 Å⁻¹, 3655 independent (*R*_{int} = 0.036) and 2996 observed reflections [*I* ≥ 2σ(*I*)], 184 refined parameters, *R* = 0.042, *wR*² = 0.091, maximum residual electron density 0.62 (–0.47) e Å⁻³, hydrogens calculated and refined as riding atoms.

3.5. Hydrogenation of **3c**, preparation of complex **6c**

A suspension of 320 mg (1.0 mmol) of **3c** and 30 mg Pd/C catalyst (10% Pd) in 50 ml of THF was stirred vigorously at r.t. and hydrogenated for 70 min at normal pressure using a gas-burette and filtered subsequently. Removal of the solvent from the filtrate afforded 308 mg of **6c** (*trans-6c*–*cis-6c*: 6.6:1) (95%). Recrystallization from pentane gave red crystals suitable for the X-ray crystal structure analysis, m.p.: 71 °C (DSC). *trans-6c*: ¹H-NMR (toluene-*d*₈): δ = 4.02 (m, 1H, Cp–H), 3.97 (m, 1H, Cp–H), 3.95 (m, 2H, Cp–H), 3.93 (m, 1H, Cp–H), 3.87 (m, 2H, Cp–H), 3.77 (m, 1H, Cp–H), 2.99 (dd, 1H, ³J = 10.9, 2.2 Hz, 8-H), 2.49 (m, 1H, 6-H), 2.39 (bm, 2H, 16/20-H), 2.29 (bm, 2H, 16/20-H), 2.19 (m, 1H, ²J = 13.3 Hz, ³J = 10.9, 2.2

Hz, 7-H_{ax}), 1.87 (m, 1H, ²J = 13.3 Hz, ³J = 4.6, 2.2 Hz, 7-H_{eq}), 1.49 (m, 4H, 17/19-H), 1.26 (m, 2H, 18-H), 1.05 (d, 3H, ³J = 7.3 Hz, 10-H). ¹³C{¹H}-NMR (toluene-*d*₈): δ = 92.5 (C-1), 82.1 (C-11), 71.3, 69.2, 69.0, 68.8, 68.2, 68.1, 68.0, 67.5 (C-2/C-3/C-4/C-5/C-12/C-13/C-14/C-15), 58.4 (C-8), 52.0 (C-16, C-20), 47.0 (C-7), 27.8 (C-6), 27.0 (C-17, C-19), 25.3 (C-18), 17.7 (C-10). Anal. Found: C, 70.22; H, 7.97; N, 4.26. Calc. for C₁₉H₂₅NFe (MW 323.2): C, 70.60; H, 7.80; N, 4.33%.

3.5.1. X-ray crystal structure analysis of *trans-6c*

Formula C₁₉H₂₅NFe, *M* = 323.25, yellow crystal 0.30 × 0.20 × 0.10 mm, *a* = 21.920(1), *b* = 17.402(1), *c* = 8.231(1) Å, *V* = 3139.7(4) Å³, ρ_{calc} = 1.368 g cm⁻³, μ = 9.54 cm⁻¹, empirical absorption correction via SORTAV (0.763 ≤ *T* ≤ 0.911), *Z* = 8, orthorhombic, space group *Pna*2₁ (No. 33), λ = 0.71073 Å, *T* = 198 K, ω and φ scans, 20 221 reflections collected (±*h*, ±*k*, ±*l*), [(sin θ)/λ] = 0.65 Å⁻¹, 6404 independent (*R*_{int} = 0.054) and 4508 observed reflections [*I* ≥ 2σ(*I*)], 381 refined parameters, *R* = 0.041, *wR*² = 0.077, maximum residual electron density 0.31 (–0.39) e Å⁻³, Flack parameter –0.02(2), two almost identical independent molecules in the asymmetric unit, hydrogens calculated and refined as riding atoms.

3.6. Preparation of complex **6d** by an amine exchange reaction

Methyliodide (4 ml, 64 mmol) was added to a solution of 0.28 g (1.0 mmol) of **6a** in 8 ml of acetonitrile and stirred for 1 h at r.t. Under reduced pressure the reaction mixture was concentrated to 2 ml, and 4 ml of MeCN and 2.5 ml of pyrrolidine (30 mmol) were added. The reaction mixture was refluxed for 16 h, evaporated to dryness and the residue dissolved in pentane. The precipitate formed was removed by filtration and the solvent evaporated from the clear orange filtrate to yield 0.29 g of orange crystals of **6d** (*trans-6d*–*cis-6d* = 6.7:1) (93%), m.p.: 84 °C (DSC). Crystals suitable for X-ray crystal structure analysis were grown from pentane. *trans-6d*: ¹H-NMR (CD₂Cl₂): δ = 4.28 (m, 1H, Cp–H), 4.12 (m, 1H, Cp–H), 4.11 (m, 1H, Cp–H), 4.05 (m, 1H, Cp–H), 4.02 (m, 1H, Cp–H), 4.00 (bm, 2H, Cp–H), 3.96 (m, 1H, Cp–H), 2.90 (dd, 1H, ³J = 2.5, 9.5 Hz, 8-H), 2.66 (m, 1H, ³J = 7.3, 5.5, 3.3 Hz, 6-H), 2.56 (m, 2H, 16/19-H), 2.49 (m, 2H, 16/19-H), 2.29 (m, 1H, ²J = 13.5 Hz, ³J = 9.5, 3.3 Hz, 7-H_{ax}), 2.21 (m, 1H, ²J = 13.5 Hz, ³J = 5.5, 2.5 Hz, 7-H_{eq}), 1.72 (m, 4H, 17/18-H), 1.23 (d, 3H, ³J = 7.3 Hz, 10-H). ¹³C{¹H}-NMR (CD₂Cl₂): δ = 92.2 (C-1), 86.7 (C-11), 70.2, 69.1, 69.0, 68.9, 68.0, 67.9, 67.8, 67.7 (C-2/C-3/C-4/C-5/C-12/C-13/C-14/C-15), 58.0 (C-8), 53.2 (C-16/C-19), 48.3 (C-7), 27.1 (C-6), 23.8 (C-17/C-18), 18.3 (C-10). HRMS (ESI) Found: 310.1252. calcd. for **6d**·H⁺ (C₁₈H₂₄NFe): 310.1258.

3.6.1. X-ray crystal structure analysis of *trans*-6d

Formula $C_{18}H_{23}NFe$, $M = 309.22$, yellow crystal $0.20 \times 0.15 \times 0.10$ mm, $a = 6.066(1)$, $b = 10.704(1)$, $c = 11.695(1)$ Å, $\alpha = 94.48(1)$, $\beta = 102.63(1)$, $\gamma = 94.55(1)^\circ$, $V = 735.1(2)$ Å³, $\rho_{\text{calc}} = 1.397$ g cm⁻³, $\mu = 10.15$ cm⁻¹, empirical absorption correction via SORTAV ($0.823 \leq T \leq 0.905$), $Z = 2$, triclinic, space group $P\bar{1}$ (No. 2), $\lambda = 0.71073$ Å, $T = 198$ K, ω and φ scans, 6671 reflections collected ($\pm h$, $\pm k$, $\pm l$), $[(\sin \theta)/\lambda] = 0.66$ Å⁻¹, 3420 independent ($R_{\text{int}} = 0.034$) and 2872 observed reflections [$I \geq 2\sigma(I)$], 182 refined parameters, $R = 0.037$, $wR^2 = 0.073$, maximum residual electron density 0.34 (-0.37) e Å⁻³, hydrogens calculated and refined as riding atoms.

Data sets were collected with a Nonius KappaCCD diffractometer, equipped with a rotating anode generator Nonius FR591. Programs used: data collection COLLECT (Nonius B.V., 1998), data reduction Denzo-SMN [26], absorption correction SORTAV [27,28], structure solution SHELXS-97 [29], structure refinement SHELXL-97 [30], graphics SCHAKAL [31].

4. Supplementary material

Crystallographic data for structural analysis have been deposited with the Cambridge Crystallographic Data Centre, CCDC nos. 156790–156795. Copies of this information may be obtained free of charge from The Director, CCDC, 12 Union Road, Cambridge, CB2 1EZ, UK (Fax: +44-1223-336033; e-mail: deposit@ccdc.cam.ac.uk or www: <http://www.ccdc.cam.ac.uk>).

Acknowledgements

Financial support from the Fonds der Chemischen Industrie and the Deutsche Forschungsgemeinschaft is gratefully acknowledged.

References

- [1] A. Togni, T. Hayashi (Eds.), *Ferrocenes: Homogeneous Catalysis*, Organic Synthesis, Materials Science, VCH, Weinheim, 1995.
- [2] (a) A. Mernyi, C. Kratky, W. Weissensteiner, M. Widhalm, *J. Organomet. Chem.* 508 (1996) 209; (b) F. Gómez-de la Torre, F.A. Jalón, A. López-Agenjo, B.R. Manzano, A. Rodríguez, T. Sturm, W. Weissensteiner, M. Martínez-Ripoll, *Organometallics* 17 (1998) 4634; (c) F.A. Jalón, A. López-Agenjo, B.R. Manzano, M. Moreno-Lara, A. Rodríguez, T. Sturm, W. Weissensteiner, *J. Chem. Soc. Dalton Trans.* (1999) 4031.
- [3] T. Sturm, W. Weissensteiner, K. Mereiter, T. Kégl, G. Jeges, G. Petöly, L. Kollár, *J. Organomet. Chem.* 595 (2000) 93.
- [4] E.M. Caynela, L. Xiao, T. Sturm, B.R. Manzano, F.A. Jalón, W. Weissensteiner, *Tetrahedron: Asymmetry* 11 (2000) 861.
- [5] S. Allenmark, A. Grundström, *Chem. Scr.* 4 (1973) 69.
- [6] G. Tainturier, K. Chhor y Sok, B. Gautheron, *C.R. Acad. Sci. Paris C* (1973) 1269.
- [7] (a) M. Rosenblum, A.K. Banerjee, N. Danieli, R.W. Fish, V. Schlatter, *J. Am. Chem. Soc.* 85 (1963) 316; (b) P. Dixneuf, *Tetrahedron Lett.* (1971) 1561; (c) P. Dixneuf, R. Dabard, *Bull. Soc. Chim. Fr.* 7 (1972) 2847.
- [8] (a) S. Knüppel, R. Fröhlich, G. Erker, *J. Organomet. Chem.* 586 (1999) 218; (b) S. Knüppel, R. Fröhlich, G. Erker, *J. Organomet. Chem.* 595 (2000) 307.
- [9] (a) M. Sališova, Š. Toma, E. Soľčániová, *Collect. Czech. Chem. Commun.* 45 (1980) 1290; (b) Y. Omote, R. Kobayashi, Y. Nakada, N. Sugiyama, *Bull. Chem. Soc. Jpn.* 46 (1973) 3315; (c) C.R. Hauser, C.E. Cain, *J. Org. Chem.* 23 (1958) 1142; (d) C.E. Cain, T.A. Mashburn, C.R. Hauser, *J. Org. Chem.* 26 (1961) 1030; (e) C.R. Hauser, T.A. Mashburn, *J. Org. Chem.* 26 (1961) 1795.
- [10] Reviews: Fe organic compounds, *Gmelin Handbook of Inorganic Chemistry*, 8th ed., vol. A8, Springer-Verlag, Berlin, 1986; B.W. Rockett, G. Marr, *J. Organomet. Chem.* 416 (1991) 327 and preceding annual reviews by these authors.
- [11] W.A. White, H. Weingarten, *J. Org. Chem.* 32 (1967) 213.
- [12] (a) S. Knüppel, G. Erker, R. Fröhlich, *Angew. Chem.* 111 (1999) 2048; (b) S. Knüppel, G. Erker, R. Fröhlich, *Angew. Chem. Int. Ed. Engl.* 38 (1999) 1923.
- [13] (a) S.-D. Bai, X.-H. Wei, J.-P. Guo, D.-S. Liu, Z.-Y. Zhou, *Angew. Chem.* 111 (1999) 2051; (b) S.-D. Bai, X.-H. Wei, J.-P. Guo, D.-S. Liu, Z.-Y. Zhou, *Angew. Chem. Int. Ed. Engl.* 38 (1999) 1927.
- [14] (a) M. Rosenblum, R.B. Woodward, *J. Am. Chem. Soc.* 80 (1958) 5443; (b) See also: A.N. Nesmeyanov, E.V. Leonova, N.S. Kochetkova, A.I. Malkova, *J. Organomet. Chem.* 96 (1975) 271.
- [15] (a) K. Hafner, G. Schultz, K. Wagner, *Chem. Ber.* 768 (1964) 539; (b) K. Hafner, K.H. Vöpel, G. Ploss, C. König, *Organic Synthesis*, Collect. vol. 5, Wiley, New York, 1973, p. 431.
- [16] (a) S. Knüppel, Doctoral dissertation, Universität Münster, 1999; (b) See also: L. Duda, G. Erker, R. Fröhlich, F. Zippel, *Eur. J. Inorg. Chem.* (1998) 1153.
- [17] (a) K.L. Brown, L. Damm, J.D. Dunitz, A. Eschenmoser, R. Hobi, C. Kratky, *Helv. Chim. Acta* 61 (1978) 3108; (b) A.G. Cook, in: A.G. Cook (Ed.), *Enamines: Synthesis, Structure, and Reactions*, 2nd ed., Marcel Dekker, New York, 1988, pp. 1–101 (and references cited therein).
- [18] (a) See for a comparison: D. Kowalski, R. Fröhlich, G. Erker, *Z. Naturforsch. B* 51 (1996) 1053; (b) G. Erker, R. Pfaff, D. Kowalski, E.-U. Würthwein, C. Krüger, R. Goddard, *J. Org. Chem.* 58 (1993) 6771; (c) G. Erker, R. Pfaff, C. Krüger, M. Nolte, R. Goddard, *Chem. Ber.* 125 (1992) 1699.
- [19] E.L. Eliel, S.H. Wilen, *Stereochemistry of Organic Compounds*, Wiley, New York, 1994, pp. 762–769, and references cited therein.
- [20] H. Günther, *NMR-Spektroskopie*, Thieme Verlag, Stuttgart, 1992.
- [21] (a) T. Hayashi, T. Mise, M. Fukushima, M. Kagotani, N. Nagashima, Y. Hamada, A. Matsumoto, S. Kawakami, M. Konishi, K. Yamamoto, M. Kumada, *Bull. Chem. Soc. Jpn.* 53 (1980) 1138; (b) C. Ganter, T. Wagner, *Chem. Ber.* 128 (1995) 1157.

- [22] (a) D. Marquarding, H. Klusacek, G. Gokel, P. Hoffmann, I. Ugi, *J. Am. Chem. Soc.* 92 (1970) 5389;
(b) G.W. Gokel, D. Marquarding, I. Ugi, *J. Org. Chem.* 37 (1972) 3052.
- [23] A. Togni, C. Breutel, A. Schnyder, F. Spindler, H. Landert, A. Tijani, *J. Am. Chem. Soc.* 116 (1994) 4062.
- [24] (a) K. Chhor y Sok, G. Tainturier, B. Gautheron, *Tetrahedron Lett.* 25 (1974) 2207;
(b) K. Chhor y Sok, G. Tainturier, B. Gautheron, *J. Organomet. Chem.* 132 (1977) 173.
- [25] S. Braun, K.-O. Kalinowski, S. Berger, *150 and More Basic NMR Experiments*, VCH, Weinheim, 1998 (and references therein).
- [26] Z. Otwinowski, W. Minor, *Methods Enzymol.* 276 (1997) 307.
- [27] R.H. Blessing, *Acta Crystallogr. A* 51 (1995) 33–37.
- [28] R.H. Blessing, *J. Appl. Crystallogr.* 30 (1997) 421.
- [29] G.M. Sheldrick, *Acta Crystallogr. A* 46 (1990) 467.
- [30] G.M. Sheldrick, *Universität Göttingen, Göttingen*, 1997.
- [31] E. Keller, *Universität Freiburg*, 1997.